

Control-Oriented Modeling and Analysis of Automotive Transcritical AC System Dynamics

Bryan Rasmussen, Andrew Alleyne^{*}, Clark Bullard, Pega Hrnjak, Norman Miller
Department of Mechanical & Industrial Engineering
University of Illinois at Urbana-Champaign
Urbana, IL 61801

ABSTRACT

This paper presents a dynamic model of a transcritical air-conditioning system, specifically suited for multivariable controller design. The physically based model retains sufficient detail to accurately predict system dynamic response while also being simple enough to be of value in determining appropriate control strategies. The control focus would be quasi-steady transitions between operating states by modulating flow rates of both air and refrigerant to meet changing constraints on capacity, efficiency, noise, etc. Both nonlinear and linearized versions of the model are compared to experimental data. Possibilities for model order reduction are substantiated.

1 INTRODUCTION

Recently, more attention has been given to replacing traditional automotive vapor compression cycle refrigerants with carbon dioxide. The advantages include:

- Carbon dioxide is a natural fluid, and does not have the negative environmental impacts of traditional refrigerants.
- The system has higher efficiencies at lower ambient temperatures [9].
- The system operates on a transcritical cycle in heat pumping or air-conditioning mode [3].
- Transcritical systems have an extra degree of freedom to trade efficiency for capacity [8][10].

The dynamics of a CO₂ vapor compression system are unique because of the transcritical nature of the cycle. The ability to accurately model these dynamics is important for both component design and system controller design.

Air-conditioning systems have traditionally been controlled using simple Single-Input Single-Output (SISO) techniques. However, research has demonstrated that this approach has numerous difficulties, and results in performance inferior to Multi-Input Multi-Output (MIMO) control strategies [6]. Furthermore, MIMO control strategies are necessary to achieve multiple objectives, such as: temperature, humidity, capacity, efficiency, etc. Development of such strategies requires extensive testing, or a simple, accurate, physically based model. Various approaches have been used to simulate the dynamic response of both subcritical and transcritical systems.

However, many of these are mathematically intractable, and of limited use for model-based multivariable controller design. Thus, a dynamic system model is needed that balances model fidelity with model simplicity. This is the primary motivation for the work presented here.

The remainder of this paper is organized as follows. In Section 2 the past modeling efforts for both subcritical and transcritical systems are described. Section 3 gives a basic description of the system to be modeled. In Section 4 the modeling approach is explained, and specific modeling results for each component are presented. Section 5 details the procedure for obtaining a local linearization of the model. Comparisons of the nonlinear and linearized version of the model with experimental data are detailed in Section 6. Construction of an empirical model using system identification techniques is presented in Section 7. Concluding remarks and an outline for future work are given in Section 8.

2 PAST MODELING EFFORTS

SUBCRITICAL SYSTEMS – Dynamic modeling of subcritical vapor compression systems has received a fair bit of attention. Various approaches have been suggested, and these can generally be placed in two categories: finite difference models and lumped parameter models. The finite difference approach results in a large number of equations suitable only for numerical simulation. The lumped parameter approach results in fewer equations, but frequently ignores important dynamics due to the complex heat exchanger behavior. Specifically, the entire evaporator is often modeled as a single lumped subsystem, which ignores the important dynamics associated with the moving boundary between the two-phase flow region and the single-phase flow region. Previously, a solution was found by developing a lumped parameter model with a moving interface boundary. This approach has been used by several authors for simulation purposes [4][5][7], and occasionally for control analysis purposes [2]. He et al. in [6] proposed extending this approach to multivariable controller design. They modeled a simple four-component subcritical cycle, and demonstrated that the model accurately predicted the important system dynamics. They also showed that this model could be simplified further, and still predict the system response correctly. This model was then used for

^{*} corresponding author: alleyne@uiuc.edu

controller design, and demonstrated the superiority of MIMO control strategies.

TRANSCRITICAL SYSTEMS - In contrast, dynamic modeling of transcritical systems has received little attention. Recent efforts [12] have generally focused on steady state performance for system optimization purposes. As with several investigations into subcritical system characterization, attempts to model the dynamics of these transcritical cycles generally employ the finite difference approach [11] and are unsuitable for controller design.

3 SYSTEM DESCRIPTION

A typical transcritical air-conditioning system consists of the five components shown in Figure 1. For a more complete description of the working principles of this system, see [9]. Unique aspects of this system include the internal heat exchanger that increases the inherently coupled nature of the dynamics, and the supercritical state of the refrigerant in the gas cooler.

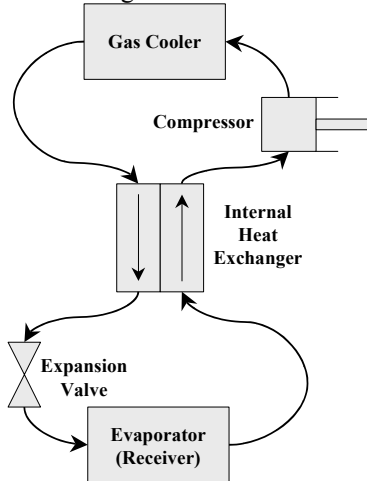


Figure 1: Diagram of Transcritical Vapor Compression Cycle

The four controllable inputs to the system are assumed to be compressor speed, expansion valve opening, and mass flow rates of air across the evaporator and gas cooler. The outputs of interest are superheat temperature (measure of efficiency), evaporator outlet air temperature (measure of comfort), as well as the operating pressures and mass flow rates. For automotive systems, it is sufficient to evaluate the system dynamics at three operating conditions, designated as idle, city, and highway. These names refer to the general conditions of compressor speed and air-flow rates encountered during engine idling, city and highway driving conditions.

4 MODELING APPROACH

Each of the five components is modeled separately and then combined to form the overall system model. The component models are divided into two groups. The compressor and valve are assumed to act instantaneously and are modeled with algebraic relationships. The heat

exchangers are modeled using a lumped parameter approach. Specifically, the models of the evaporator and gas cooler are obtained by using the PDEs for the conservation of mass and energy for fluid flow in a tube. These equations are integrated along the length of the heat exchanger to remove spatial dependence. This approach has been used previously to model subcritical system components in [4] and [6]. The resulting set of equations is a 9th order, lumped-parameter model for a transcritical air-conditioning system.

The following subsections will discuss the models for the individual components.

EVAPORATOR – The evaporator is modeled as one-dimensional fluid flow in a tube with effective parameters of length, diameter, and inner and outer surface areas. Axial conduction of refrigerant is assumed to be negligible, and the refrigerant pressure along the entire heat exchanger tube is assumed to be uniform.

$$\frac{\partial \rho A}{\partial t} + \frac{\partial \dot{m}}{\partial z} = 0 \quad (1)$$

$$\frac{\partial(\rho A h - A P)}{\partial t} + \frac{\partial(\dot{m} h)}{\partial z} = \pi D_i \alpha_i (T_w - T_r) \quad (2)$$

$$(C_p \rho A)_w \frac{\partial T_w}{\partial t} = \pi D_i \alpha_i (T_r - T_w) + \pi D_o \alpha_o (T_a - T_w) \quad (3)$$

$$\int_{z_1(t)}^{z_2(t)} \frac{\partial f(z, t)}{\partial t} dz = \frac{d}{dt} \left[\int_{z_1(t)}^{z_2(t)} f(z, t) dz \right] - f(z_2(t), t) \frac{d(z_2(t))}{dt} + f(z_1(t), t) \frac{d(z_1(t))}{dt} \quad (4)$$

Equations 1-2 are the conservation of refrigerant mass and energy for fluid flow in a tube. Equation 3 is the conservation of tube wall energy. These equations are integrated using Equation 4 to remove spatial dependence and yield several coupled ODEs. The limits of integration depend on the operating condition being considered. For the evaporator model, three conditions need to be considered.

Condition 1 – First consider the condition when fluid enters the evaporator as a two-phase fluid, exits as a superheated vapor, and the receiver is either completely filled with superheated vapor or nonexistent (Figure 2). The model for this condition has been developed previously by He et al in [6] and used for the modeling of a subcritical cycle. In this case the evaporator is divided into two regions: a two-phase region, and a superheated region. The model developed in [6] assumes a constant mean void fraction in the two-phase region, which has been shown to be valid for most quasi-steady transitions [1]. Following the same derivation approach, but assuming a time varying mean void fraction results in an alternative model. Although this added complexity is arguably unnecessary for an evaporator in this operating condition, it is essential for future models of evaporators that operate without a superheat region (i.e. evaporator with receiver).

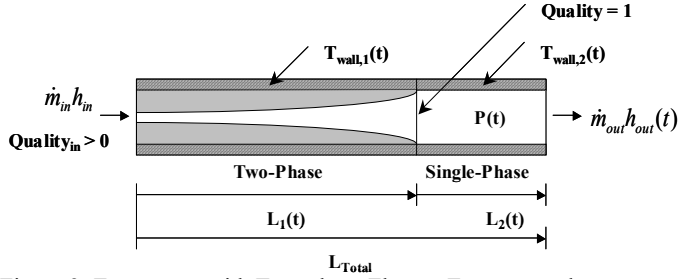


Figure 2: Evaporator with Two-phase Flow at Entrance and Superheated Vapor at Exit

Condition 2 – Next consider the condition when the fluid enters as a two-phase fluid, exits as a superheated vapor, but the receiver contains both liquid and vapor fluid. This is a non-equilibrium condition, and is not considered in this paper. However, the evaporator model would be identical to the model for the first condition, and the receiver model for this condition was developed by Grald and MacArthur in [4].

Condition 3 – Finally consider the condition when the fluid enters and exits the evaporator as a two-phase fluid, and the receiver contains both liquid and vapor fluid. This condition is not considered in this paper, but will be the subject of future studies.

A partial derivation for an evaporator in Condition 1 is presented here. After integrating to remove spatial dependence, and assuming a time varying mean void fraction, the following equations result. For explanation of the notation, see the Appendix.

The conservation of refrigerant mass is shown in Equations 5 and 6.

$$\left[\frac{\partial \rho_f}{\partial P} (1 - \bar{\gamma}) + \frac{\partial \rho_g}{\partial P} (\bar{\gamma}) \right] A_{cs} L_1 \dot{P} + [\rho_g - \rho_f] A_{cs} L_1 \dot{\bar{\gamma}} + [(\rho_f - \rho_g)(1 - \bar{\gamma})] A_{cs} \dot{L}_1 + \dot{m}_{int} - \dot{m}_i = 0 \quad (5)$$

$$\left[\frac{\partial \rho_2}{\partial P} + \frac{1}{2} \frac{\partial \rho_2}{\partial h_2} \frac{\partial h_g}{\partial P} \right] A_{cs} L_2 \dot{P} + \left[\frac{1}{2} \frac{\partial \rho_2}{\partial h_2} \right] A_{cs} L_2 \dot{h}_o + [\rho_g - \rho_2] A_{cs} \dot{L}_1 + \dot{m}_o - \dot{m}_{int} = 0 \quad (6)$$

The conservation of refrigerant energy is shown in Equations 7 and 8.

$$\left[\frac{\partial(\rho_f h_f)}{\partial P} (1 - \bar{\gamma}) + \frac{\partial(\rho_g h_g)}{\partial P} (\bar{\gamma}) - 1 \right] A_{cs} L_1 \dot{P} + [(\rho_f h_f - \rho_g h_g)(1 - \bar{\gamma})] A_{cs} \dot{L}_1 + [\rho_g h_g - \rho_f h_f] A_{cs} L_1 \dot{\bar{\gamma}} + \dot{m}_{int} h_g - \dot{m}_i h_i = \alpha_{i1} A_i \left(\frac{L_1}{L_{Total}} \right) (T_{w1} - T_{r1}) \quad (7)$$

$$\left[\left(\frac{\partial \rho_2}{\partial P} + \frac{1}{2} \frac{\partial \rho_2}{\partial h_2} \frac{\partial h_g}{\partial P} \right) h_2 + \frac{\rho_2}{2} \frac{\partial h_g}{\partial P} - 1 \right] A_{cs} L_2 \dot{P} + [\rho_g h_g - \rho_2 h_2] A_{cs} \dot{L}_1 + \left[\frac{1}{2} \frac{\partial \rho_2}{\partial h_2} h_2 + \frac{\rho_2}{2} \right] A_{cs} L_2 \dot{h}_o + \dot{m}_o h_o - \dot{m}_{int} h_g = \alpha_{i2} A_i \left(\frac{L_2}{L_{Total}} \right) (T_{w2} - T_{r2}) \quad (8)$$

Conservation of heat exchanger wall energy is shown in Equations 9 and 10.

$$(C_p \rho V)_w \dot{T}_{w1} = \alpha_{i1} A_i (T_{r1} - T_{w1}) + \alpha_o A_o (T_a - T_{w1}) \quad (9)$$

$$(C_p \rho V)_w \left(\dot{T}_{w2} + \frac{T_{w1} - T_{w2}}{L_2} \dot{L}_1 \right) = \alpha_{i2} A_i (T_{r2} - T_{w2}) + \alpha_o A_o (T_a - T_{w2}) \quad (10)$$

These equations can be combined to eliminate the variable denoting the intermediate mass flow rate. Mean void fraction is reformulated as a function of the state and input variables. The resulting five equations are combined into the nonlinear state space format shown in Equation 11, where the state and input vectors are defined in Equations 12 and 13.

$$D(x, u) \cdot \dot{x} = f(x, u) \quad (11)$$

$$x = [L_1 \quad P \quad h_o \quad T_{w1} \quad T_{w2}]^T \quad (12)$$

$$u = [\dot{m}_i \quad \dot{m}_o \quad h_i \quad \dot{h}_i \quad T_{air, in} \quad \dot{m}_{air}]^T \quad (13)$$

GAS COOLER – The gas cooler is modeled similarly to the evaporator. The conservation equations are applied and reduced to ODEs. Because the fluid is in a supercritical state while in the gas cooler, the gas cooler is treated as one single-phase region (Figure 4).

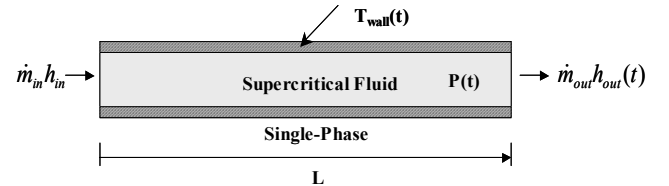


Figure 3: Gas Cooler with a Single Region of Supercritical Fluid

The resulting equations are given. The conservation of refrigerant mass is shown in Equation 14. The conservation of refrigerant energy is shown in Equation 15. The conservation of heat exchanger wall energy is shown in Equation 16.

$$\left(\frac{\partial \rho}{\partial P} \right) A_{cs} L \dot{P} + \left(\frac{\partial \rho}{\partial h} \right) \frac{A_{cs} L}{2} \dot{h}_i + \left(\frac{\partial \rho}{\partial h} \right) \frac{A_{cs} L}{2} \dot{h}_o + \dot{m}_o - \dot{m}_i = 0 \quad (14)$$

$$\left(\frac{\partial \rho}{\partial P} h_{ave} + 1 \right) A_{cs} L \dot{P} + \left(\frac{\partial \rho}{\partial h} h_{ave} + \rho_{ave} \right) \left(\frac{A_{cs} L}{2} \right) (\dot{h}_i + \dot{h}_o) + \dot{m}_o h_o - \dot{m}_i h_i = \alpha_i A_i (T_w - T_r) \quad (15)$$

$$\alpha_i A_i (T_r - T_w) + \alpha_o A_o (T_a - T_w) = (C_p \rho V)_w \dot{T}_w \quad (16)$$

As with the evaporator, these equations can be arranged in the form of Equation 11, where the state vector is defined in Equation 17, and the input vector defined identically to the evaporator in Equation 13.

$$x = [P \quad h_o \quad T_w]^T \quad (17)$$

INTERNAL HEAT EXCHANGER – The internal heat exchanger is modeled with a single ordinary differential equation based on a lumped capacitance assumption, and two algebraic constraints (Equations 18-20). The energy difference between the entering and exiting fluids is assumed to be equal to that entering the heat exchanger wall (Equations 18-19). The wall of the heat

exchanger is modeled with a lumped thermal capacitance which governs the rate of energy storage (Equation 20).

$$\dot{m}_h(h_{h,in} - h_{h,out}) = \alpha_h A_h (T_{h,ave} - T_{wall}) \quad (18)$$

$$\dot{m}_c(h_{c,in} - h_{c,out}) = \alpha_c A_c (T_{c,ave} - T_{wall}) \quad (19)$$

$$\alpha_c A_c (T_{c,ave} - T_{wall}) + \alpha_h A_h (T_{h,ave} - T_{wall}) = (\rho V C_p)_{wall} \dot{T}_{wall} \quad (20)$$

$$\dot{m}(h_{in} - h_{out}) \approx \dot{m} C_p (T_{in} - T_{out}) \quad (21)$$

To simplify this system of Differential Algebraic Equations (DAEs), an approximation for the enthalpy difference is used (Equation 21).

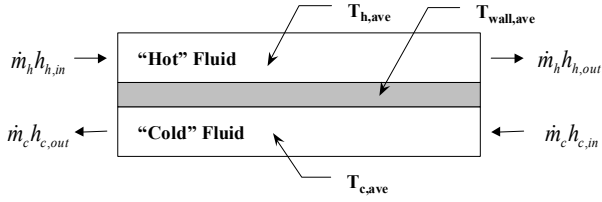


Figure 4: Diagram of a Counterflow Heat Exchanger

COMPRESSOR – The compressor is modeled as a static component. Mass flow rate is calculated using Equation 22. The expression in brackets represents the volumetric efficiency of the compressor, where C_k , D_k , and n are empirical parameters.

$$\dot{m}_k = \omega_k V_k \rho_k \left[1 + C_k - D_k \left(\frac{P_{out}}{P_{in}} \right)^{\frac{1}{n}} \right] \quad (22)$$

Furthermore, the compressor is assumed to be adiabatic, and an isentropic efficiency is used to relate inlet and outlet enthalpies (Equation 23).

$$\frac{h_{out,isentropic} - h_{in}}{h_{out} - h_{in}} = \eta_k \quad (23)$$

EXPANSION VALVE – The expansion valve is also modeled as a static component. Mass flow rate is calculated using Equation 24. Additionally, the valve is assumed to be isenthalpic (Equation 25).

$$\dot{m}_v = C_v A_v \sqrt{\rho_v (P_{in} - P_{out})} \quad (24)$$

$$h_{in} = h_{out} \quad (25)$$

5 MODEL LINEARIZATION

A classical approach is followed to obtain a linearized version of the model suitable for dynamic analysis and controller design. A Taylor's series expansion is used where 2nd order and higher order terms are omitted and deviation variables are introduced (Equation 26). For the evaporator and gas cooler an additional assumption is made. The 'D' matrix in Equation 11 is assumed to remain constant about an operating condition, and the linearization

can be simplified greatly. The resulting equation would be of the form of Equation 27.

$$\delta x = x - x_o \quad \delta u = u - u_o \quad (26)$$

$$\delta \tilde{x} = \underbrace{\left[D \Big|_{x_o, u_o} \right]^{-1}}_A \left[\frac{\partial f}{\partial x} \Big|_{x_o, u_o} \right] \delta x + \underbrace{\left[D \Big|_{x_o, u_o} \right]^{-1}}_B \left[\frac{\partial f}{\partial u} \Big|_{x_o, u_o} \right] \delta u \quad (27)$$

Space constraints will not allow a complete exposition of the linearized system. However, the numerical values for the A and B matrices for the evaporator and gas cooler evaluated at a specific operating condition are included (Tables 2-5). This operating condition was selected to imitate highway-driving conditions while ensuring that the evaporator was operating within the restrictions of Condition 1. The operating condition is detailed in Table 1. SI units of [kg], [s], [m], [C], [kPa], and [kJ] are used.

Table 1: Highway Operating Condition

Compressor Speed	1800 [rpm]
Evaporator Air Flow Rate	300 [cfm]
Gas Cooler Air Flow Rate	2000 [cfm]
Indoor Ambient Temperature	32 [C]
Outdoor Ambient Temperature	50 [C]

Table 2: Evaporator 'A' Matrix

-0.97	0.07	0.02	-6.20	-0.04
-2,423.37	-125.55	-400.90	10,458.74	887.29
-888.72	-2.84	-81.62	49.24	180.65
-0.11	0.06	0.00	-5.99	-0.03
-13.99	0.98	0.48	-88.63	-1.46

Table 3: Evaporator 'B' Matrix

37.80	14.70	-0.03	0.05	0.00	0.00
184,777.57	-312,042.64	43.53	-124.04	0.00	0.00
5,775.73	-14,722.82	0.20	-1.48	0.00	0.00
0.00	0.00	0.00	0.00	0.06	10.73
541.04	210.37	-0.37	0.67	0.06	7.81

Table 4: Gas Cooler 'A' Matrix

-20.95	-432.91	3,487.55
-0.81	-16.71	134.64
0.00	0.06	-0.71

Table 5: Gas Cooler 'B' Matrix

621,611.43	-241,221.97	-1,281.09	0.00	0.00	0.00
3,182.60	11,502.27	-49.46	-1.00	0.00	0.00
0.00	0.00	0.24	0.00	0.10	-2.08

Furthermore, the singular values of these components indicate that a simpler physically based model could be obtained with a lower order model (Table 6).

Table 6: Evaporator and Gas Cooler Singular Values

Evaporator			Gas Cooler		
Idle	City	Highway	Idle	City	Highway
6844.37	6977.59	10784.23	2377.25	3452.45	3517
322.71	478.49	872.81	0.02	0.04	0.03
0.62	1.13	0.91	0	0	0
0.04	0.09	0.05			
0	0	0			

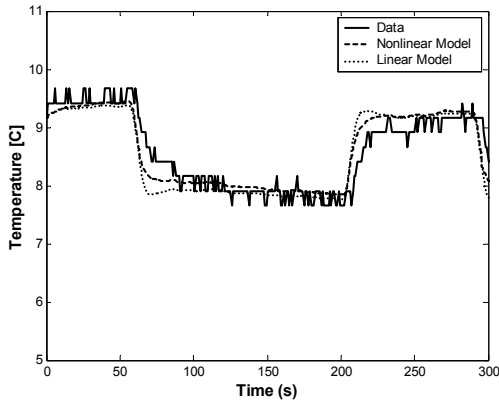


Figure 5: Evaporator Exit Air Temperature for Step Changes in Compressor Speed

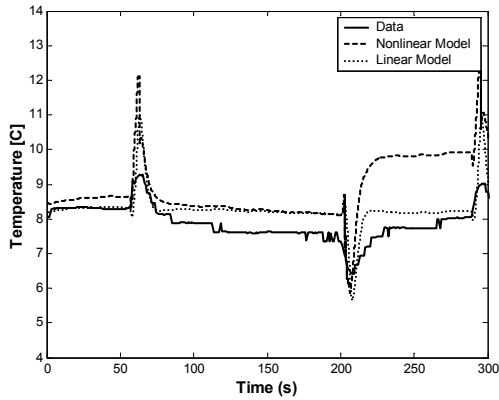


Figure 6: Superheat Temperature for Step Changes in Compressor Speed

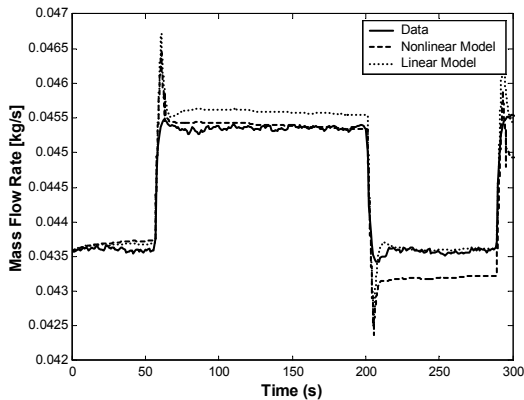


Figure 7: Mass Flow Rate for Step Changes in Compressor Speed

6 MODEL VALIDATION

To validate the modeling approach, a test facility [9] is used to record transient system responses based on changes in control inputs. A pseudo-random binary sequence is applied to each of the four controllable inputs individually and also simultaneously. The transient data is compared to simulated results for both the nonlinear and linearized versions of the model in Figures 5-7. The data is shown for the operating condition defined in Table 1.

The comparison between simulation results and experimental data shows partial agreement. The predicted evaporator exit air temperature dynamics are slightly faster than measured values, but agree in steady state value (Figure 5). The dynamic response of evaporator superheat matches in form but not in magnitude (Figure 6). In fact, the measured superheat response appears to be a filtered version of the simulated superheat response. This difference is likely caused by the differences between actual and modeled heat exchanger geometry. The discrepancy between predicted and measured mass flow rate is likely due to sensor dynamics (Figure 7).

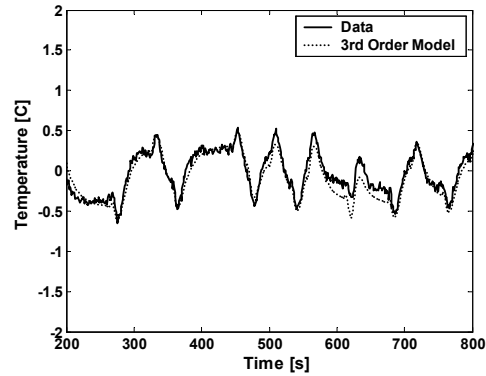


Figure 8: Evaporator Superheat for Step Changes in Expansion Valve Opening

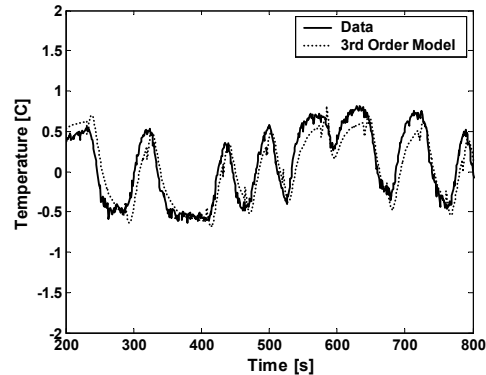


Figure 9: Evaporator Superheat for Step Changes in Compressor Speed

7 SYSTEM IDENTIFICATION

The data obtained from the transient tests is also used to develop an empirical dynamic model. System identification techniques are used to analyze the data offline

to develop a linear low-order model. First, desired outputs are selected as the evaporator superheat temperature and evaporator exit air temperature, and inputs are selected as the four controllable inputs listed previously. Second, discrete-time ARMAX models of various orders are used to construct transfer functions for each input-output pair. By inspection of the RMS error for each order of transfer function the maximum order necessary is determined. A transfer function matrix is constructed from the individual transfer functions, and then converted into state-space form. Model reduction techniques are used to eliminate redundant information.

The preliminary results from the empirical model demonstrate that the system can accurately be modeled as a 3rd order system, instead of the 9th order system predicted by the physical model (Figures 8-9). This agrees with the analysis of the singular values of the linearized model. Thus, the physically based model could possibly be reduced further without loss of accuracy.

8 CONCLUSION

In this paper a modeling approach for transcritical air-conditioning dynamics was presented. The modeling approach was validated using data from an experimental system available at UIUC. The singular values of the linearized model and preliminary system identification results indicate further simplification of the model is possible without compromising model fidelity. Future work will explore the dominant system dynamics and possibilities for reduced-order models, as well as different multivariable controller strategies.

ACKNOWLEDGMENTS

The authors would like to acknowledge the financial and technical support of the sponsoring companies of the Air-Conditioning and Refrigeration Center at the University of Illinois at Urbana-Champaign.

REFERENCES

1. Beck, B.T. Wedekind, G.L., "Generalization of the System Mean Void Fraction Model for Transient Two-Phase Evaporating," *Journal of Heat Transfer-Transactions of the ASME*, Vol. 103, pp 81-85, Feb 1981.
2. Broersen, P., and van der Jagt, M., "Hunting of Evaporators Controlled by a Thermostatic Expansion Valve," *ASME Journal of Dynamic Systems, Measurement, and Control*, Vol. 102, pp. 130-135, June 1980.
3. Giannavola, M.S., Murphy, R., Yin, J.M., Kim, M-H., Bullard, C.W., and Hrnjak, P.S., "Feasibility of Transcritical CO₂ Heat Pump for a Sport Utility Vehicle," *Proceedings of the IIR Gustav Lorentzen Conference on Natural Working Fluids*, pp. 115-122, July 2000.
4. Grald, E.W., and MacArthur, J.W., "A Moving Boundary Formulation for Modeling Time-Dependent Two-Phase

- Flows," *Int. J. Heat and Fluid Flow*, Vol. 13, No. 3, pp. 266-272, 1992.
5. Gruhle, W.D., and Isermann, R., "Modeling and Control of a Refrigerant Evaporator," *ASME Journal of Dynamic Systems, Measurement, and Control*, Vol. 107, pp. 235-239, June 1980.
6. He, X., Liu, S., and Asada, H., "Modeling of Vapor Compression Cycles for Multivariable Feedback Control of HVAC Systems," *ASME J. of Dynamic Systems, Measurement, and Control*, Vol. 119, pp. 183_191, June 1997.
7. Kapadia, M., and Wolgemuth, C.H., "A Dynamic Model of a Condenser in a Closed Rankine Cycle Power Plant," *Proc. 1984 American Control Conf.*, pp. 79-84, 1984.
8. McEnaney, R.P., and Hrnjak, P.S., "Control Strategies for Transcritical R744 Systems," SAE World Congress, paper 2000-01-1272, 2000.
9. McEnaney, R.P., Park, Y.C., Yin, J.M., and Hrnjak, P.S., "Performance of the Prototype of a Transcritical R744 Mobile Air Conditioning System," SAE World Conference, Detroit, MI, SAE Paper No. 1999-01-0872, March 1998.
10. Park, Y.C., Yin, J.M., Bullard, C.W., and Hrnjak, P.S., "Experimental and Model Analysis of Control and Operating Parameters of Transcritical CO₂ Mobile Air Conditioning System," VTMS Conference, London, UK, 163-170, May 1999.
11. Pfafferott, T., and Schmitz, G., "Numeric Simulation of an Integrated CO₂ Cooling System," *Modelica Workshop 2000 Proceeding*, pp. 89-92, 2000.
12. Robinson, D., and Groll, A., "Introducing ACCO₂ – A Public Domain Air-To-Air Simulation Model of the Transcritical Carbon Dioxide Cycle," *Proceedings of the IIR Gustav Lorentzen Conference on Natural Working Fluids*, pp. 33-42, July 2000.

APPENDIX

Variable	Explanation	Subscript	Explanation
T	Temperature	f	Liquid
P	Pressure	g	Gas
h	Enthalpy	i	In; Inner
u	Internal Energy	o	Out; Outer
C _p	Specific Heat	int	Intermediate
ρ	Density	ave	Average
$\bar{\gamma}$	Mean Void Fraction	cs	Cross-Sectional
α	Heat Transfer Coefficient	r	Refrigerant
ω	Rotational Speed	w	Wall
η	Efficiency	h	Hot
\dot{m}	Mass Flow Rate	c	Cold
A	Area	v	Valve
L	Length	k	Compressor
V	Volume	rec	Receiver
C,D,n,UA	Empirical Parameters		